*Acta Cryst.* (1978) A**34**, 556–561

# Vacancy–Strain Coupling in Ordered TiO

BY H. TERAUCHI* AND J. B. COHEN

*Department of Materials Science and Engineering, The Technological Institute, Northwestern University, Evanston, IL* 60201, *USA*

AND T. B. REED†

*MIT Lincoln Laboratory, Lexington, MA* 02173, *USA*

(*Received* 7 *November* 1977; *accepted* 27 *January* 1978)

The structure of the partially ordered phase of TiO has been examined with a single crystal. While the space group is that first determined from powder X-ray diffraction and electron diffraction by Watanabe, Castle, Jostons & Malin [*Acta Cryst.* (1967). **23**, 307–313], (*B*2/*m*), the average structure is somewhat different. There are waves of Ti and O ion vacancies every third (100) plane in the [010] direction of the monoclinic structure. The amplitude of the wave is twice as large for the Ti ion vacancies as for the O ion vacancies. There is no appreciable concentration of interstitial Ti ions in either the ordered phase or the disordered (cubic) phase. The ordering temperature $T_c$ is 1026 (2)°C. The monoclinic angle is directly proportional to the square of the order parameter associated with vacancy ordering. A mean-field theory is developed that includes vacancy–vacancy and vacancy–electron interactions, and vacancy–strain coupling. This theory explains the main features of the order–disorder transition in this material.

## Introduction

The monoxides of the first transition series have structures which at first glance are all that of NaCl (*Strukturbericht* type *B*1). But there are now known to be many details which do not fit this simple description, such as interstitial metal ions, vacancy clusters and various ordered phases, often involving such clusters. For example, for TiO 14·5% of the anion and cation sites are vacant (Banus & Reed, 1970; Taylor & Doyle, 1970). Watanabe, Castle, Jostons & Malin (1967) and Watanabe, Terasaki, Jostons & Castle (1968, 1970) reported that these vacancies were ordered below ~950°C and the NaCl structure was distorted to a monoclinic system, space group *B*2/*m* (No. 12). In particular, it was proposed that half of the Ti and half of the O ions are missing every third (110) plane in the cubic phase [equivalent to every third (100) plane in the monoclinic phase]. However, this conclusion was based primarily on only 26 superlattice powder reflections and we calculated the *R* factor for these to be 0·33 from this data. A more detailed study is presented here.

In a previous paper (Terauchi & Cohen, 1977), we pointed out that the diffuse intensity present above $T_c$ implies important vacancy–vacancy and vacancy–electron interactions. But the distortion of the unit cell when the vacancies order implies that vacancy–strain coupling is also important in this system below $T_c$.

In this paper, the temperature dependence of the intensity of superlattice reflections and the monoclinic angle have been measured at high temperatures. A theory is developed for the transition that includes the above mentioned interactions; this theory describes the essential features of the transition.

## Procedures

Crystals were prepared in a purified argon atmosphere in a tri-arc furnace (Reed & Pollard, 1968). The starting materials were $TiO_2$ (99·9% pure) and Ti (99·9% pure). After melting, coarse-grained specimens were obtained, with grains of approximate size 1 × 1 × 9 mm, which were quite suitable for X-ray studies. Such specimens were homogenized at 1200°C for 2 d. The crystal employed for determining the ordered structure was annealed at 950°C for 15 h after a 15 h cool from the higher temperature. This was the same temperature employed by Watanabe *et al.* (1967). This heat treatment was chosen because when the ordered phase forms and the structure changes from cubic to monoclinic there are different domains and, furthermore, there is twinning in each domain. If the specimen is fully ordered at lower temperatures the various domains are not equal in size.

All heat treatments were carried out in helium gas (99·9% pure) flowing at 7 cm$^3$ min$^{-1}$, passed over Ti

---

[*] On leave from Kwansei Gakuin University, Nishinomiya, Japan.

[†] Present address: Solar Energy Research Institute, 536 Cole Boulevard, Golden, Colorado 80401, USA.

Table 1. *Parameters for* TiO

Space group: $B2/m$ (No. 12), $a_m = 9{\cdot}340$ (5), $b_m = 5{\cdot}860$ (4), $c_m = 4{\cdot}141$ (1) Å, $\gamma_m = 107{\cdot}553$ (6)° (weighted $\lambda = 1{\cdot}5418$ Å).

| Atom | Equipoint | Occupation factor | (000), $(\frac{1}{2}0\frac{1}{2})$ + | | | $B$(Å$^2$) | $\langle u^2\rangle^{\frac{1}{2}}$ (Å) $\times 10^2$ |
|---|---|---|---|---|---|---|---|
| | | | $x$ | $y$ | $z$ | | |
| Ti(1) | 2($a$) | 0·284 (20) | 0 | 0 | 0 | 2·756 | 3·49 |
| Ti(2) | 2($c$) | 0·941 (10) | 0 | $\frac{1}{2}$ | 0 | 1·120 | 1·42 |
| Ti(3) | 4($i$) | 0·952 (10) | 0·3360 (7) | 0·1620 (13) | 0 | 0·925 | 1·17 |
| Ti(4) | 4($i$) | 0·958 (8) | 0·3396 (6) | 0·6670 (14) | 0 | 0·852 | 1·08 |
| O(1) | 2($b$) | 0·782 (11) | 0 | $\frac{1}{2}$ | $\frac{1}{2}$ | 1·906 | 2·41 |
| O(2) | 2($d$) | 0·462 (35) | 0 | 0 | $\frac{1}{2}$ | 1·206 | 1·53 |
| O(3) | 4($i$) | 0·945 (12) | 0·1765 (24) | 0·3244 (47) | 0 | 1·152 | 1·46 |
| O(4) | 4($i$) | 0·948 (10) | 0·1642 (24) | 0·8056 (44) | 0 | 1·214 | 1·54 |

In disordered cubic phase: $B_{\mathrm{O}} = 1{\cdot}105$ Å$^2$, $B_{\mathrm{Ti}} = 0{\cdot}937$ Å$^2$.

chips maintained at 650 °C, and then through a trap at dry-ice temperatures. Cooling to room temperature involved turning off the furnace while maintaining the gas flow. At about 500 °C, specimens were removed to a cold zone just outside the furnace. Crystals were checked for weight loss and any change in the position of a high-angle peak, to verify that the composition was unchanged.

For the X-ray measurements, unless otherwise noted, a modified GE XRD-5 diffractometer with a quarter circle was employed (Schwartz, Cohen & Morrison, 1964) with an incident-beam monochromator of pyrolytic graphite, singly bent to focus the beam vertically at the receiving slits. Cu $K\alpha$ radiation in point focus, and a proportional counter with a pulse-height analyzer set for ~90% acceptance of the Cu $K\alpha$ were employed. An 8 μm thick Ni filter in front of the detector reduced the background (largely Ti fluorescence) by one third, while reducing a Bragg peak by only 12%.

Both $\omega$ and $\theta$–$2\theta$ scans were used to sample reciprocal space, but all integrations were carried out in the $\theta$–$2\theta$ mode employing a computer control (Richesson, Morrison, Cohen & Paavola, 1971) and in the $\chi = 90°$ position to avoid absorption corrections. The beam was smaller than the crystal at all positions, and the FWHM of a reflection in an $\omega$ scan was about 0·014 $a_c^*$, where $a_c^*$ is the parameter of the unit cell of reciprocal space of the disordered cubic phase. Receiving slits were opened until integrations were independent of their size. Data were corrected for surface roughness by measuring the Ti fluorescence *vs* $2\theta$ and correcting for the difference in absorption of the incoming Cu $K\alpha$ and outgoing Ti fluorescence (Suortti, 1972).

For studies of order *vs* temperature a crystal was maintained in an atmosphere of helium purified as indicated above. The furnace (Gehlen, 1969) was covered with a Be hemisphere 380 μm thick. The temperature was controlled with a feedback system to ±2·0 °C. (The thermocouples, made of platinum–platinum 13% rhodium, were checked at the boiling point of water.)

## Results

### *The partially ordered phase*

Indices in the monoclinic unit cell ($m$) are related to those in the cubic cell ($c$) by:

$$h_m = h_c + 2\,k_c, \quad k_m = h_c - k_c, \quad l_m = l_c. \qquad (1)$$

The lattice parameters of the monoclinic phase were obtained from the split 060, 111, 002 and $4\bar{2}0$ reflections. These parameters are given in Table 1; the uncertainty is estimated from errors in estimating the peak positions and the uncertainty in the true zero of the diffractometer. The monoclinic angle $\gamma$ (107·55°) is less than that between the corresponding directions $[1\bar{1}0]$ and [120] in the cubic phase by 0·85°.* Reflections were present for the diffraction symbol $112/mB$. The most symmetric space group $B2/m$ (No. 12) was chosen for least-squares refinement (Busing, Martin & Levy, 1962). The refined $R$ parameter was

$$R = \sum_i \left(|F_i^{\rm obs}| - |F_i^{\rm calc}|\right)/F_i^{\rm obs}. \qquad (2)$$

The weighted $R$ parameter was also calculated:

$$R_w = \left[\sum_i w_i(|F_i^{\rm obs}| - |F_i^{\rm calc}|)^2/\sum_i w_i|F_i^{\rm obs}|^2\right]^{1/2}. \qquad (3)$$

Here $w_i$ was taken as the inverse of the net intensity above background. At first, the temperature factors were fixed at the overall values calculated in Watanabe *et al.* (1967), and the occupancies, conversion factor and positions were refined. Then temperature factors

---

* As will be shown, $\gamma$ is very sensitive to order. As Watanabe *et al.* (1967) in their study found $\gamma = 107{\cdot}52°$, their degree of order was essentially the same as that in our specimen (which is ~0·8 at 950 °C).

Table 2. *Observed and calculated superstructure structure factors*

$R$ index: 0·104; weighted $R$ index: 0·116.

| $h_m k_m \ell_m$ | $F_{obs}$ | $F_{calc}$ | $h_m k_m \ell_m$ | $F_{obs}$ | $F_{calc}$ |
|---|---|---|---|---|---|
| 400 | 35.48 | 35.06 | 101 | 19.35 | 20.39 |
| 800 | 6.11 | 5.21 | 111 | 25.94 | 27.19 |
| 010 | 19.61 | 21.82 | 311 | 9.12 | 11.90 |
| 210 | 17.45 | 17.45 | 711 | 10.64 | 13.93 |
| 410 | 17.00 | 15.61 | $\bar{1}11$ | 26.01 | 28.97 |
| 610 | 14.42 | 11.09 | $\bar{7}11$ | 11.59 | 7.87 |
| $\bar{2}10$ | 17.96 | 20.52 | $\bar{3}21$ | 3.21 | 5.13 |
| $\bar{4}10$ | 19.85 | 16.47 | $\bar{5}21$ | 35.54 | 34.08 |
| $\bar{6}10$ | 15.21 | 12.77 | 131 | 28.16 | 26.81 |
| $\bar{8}10$ | 11.21 | 12.50 | $\bar{5}31$ | 13.67 | 16.06 |
| 020 | 39.33 | 36.07 | 212 | 14.93 | 14.29 |
| 420 | 11.44 | 11.51 | 412 | 11.66 | 12.42 |
| $\bar{2}20$ | 29.32 | 28.35 | 612 | 9.94 | 9.22 |
| 030 | 9.51 | 12.98 | $\bar{2}12$ | 12.66 | 15.15 |
| 230 | 10.33 | 14.46 | $\bar{4}12$ | 11.02 | 12.81 |
| 430 | 10.45 | 12.52 | $\bar{6}12$ | 10.90 | 11.10 |
| $\bar{2}30$ | 19.69 | 15.69 | 422 | 10.72 | 9.97 |
| $\bar{4}30$ | 18.27 | 14.91 | $\bar{2}22$ | 24.21 | 22.43 |
| $\bar{6}30$ | 13.54 | 12.88 | $\bar{6}22$ | 10.70 | 10.29 |
| $\bar{8}30$ | 7.05 | 8.51 | 032 | 10.45 | 10.53 |
| 040 | 12.88 | 13.87 | 232 | 11.71 | 11.52 |
| $\bar{4}40$ | 14.27 | 16.26 | $\bar{2}32$ | 12.72 | 12.94 |
| $\bar{6}40$ | 19.51 | 19.71 | $\bar{4}32$ | 13.04 | 12.22 |
| 050 | 11.71 | 12.58 | $\bar{6}32$ | 13.07 | 10.71 |
| $\bar{2}50$ | 12.28 | 11.42 | 042 | 12.88 | 12.53 |

were refined with the other factors fixed. Isotropic temperature factors were assumed, one for each atom type in each equipoint.* Three cases were examined: all 63 superstructure peaks and 11 fundamental peaks, the 63 superstructure peaks alone, and superstructure peaks alone, eliminating 13 superstructure reflections that were difficult to separate from peaks because of other domains or twins. The results for the last case are given in Table 1 and the structure factors in Table 2. [For the first case the $R$ index was 0·151 and $R_w$ = 0·124, for the second $R$ = 0·164, $R_w$ = 0·181. Except for the second case, the $R$ factors are what may be expected from the number of unknowns, number of peaks and the variation in intensity over the experiment (2·3%) following Hamilton (1965*a*).] In all three cases the parameters differed only by the sum of the standard deviations.

In Fig. 1, the occupancy factors of the Ti(1) and O(2) positions are plotted *vs* $R$. Also given is the 95% confidence limit (following Hamilton, 1965*b*) that the minimum values are different from the model of Watanabe *et al.* (1967). The structure is shown in Fig. 2. There are waves of vacancies in the [010] monoclinic direction, every third plane of O or Ti ions. But in contrast to Watanabe *et al.*'s (1967) result these waves do not have the same amplitude for the two ions, and there are some vacancies on planes parallel to the main wave.*

Summing the occupation factors (which were not held fixed in the refinement), the chemical formula is $TiO_{0\cdot997}$ in agreement with the value determined by combustion to the highest oxide. The vacancy concentration is 16·2 at.% for O, 15·9 at.% for Ti, compared with the value of 14·5% determined for this composition (Banus & Reed, 1970) from the lattice parameter of the cubic phase, its density and combustion.

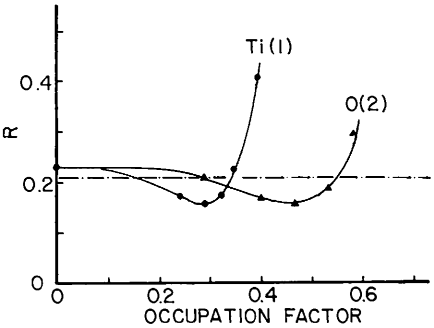

Fig. 1. $R$ index *vs* occupation factor for Ti(1) and O(2) (see Table 1). The horizontal dashed line represents the 95% confidence limit following Hamilton (1965*b*).

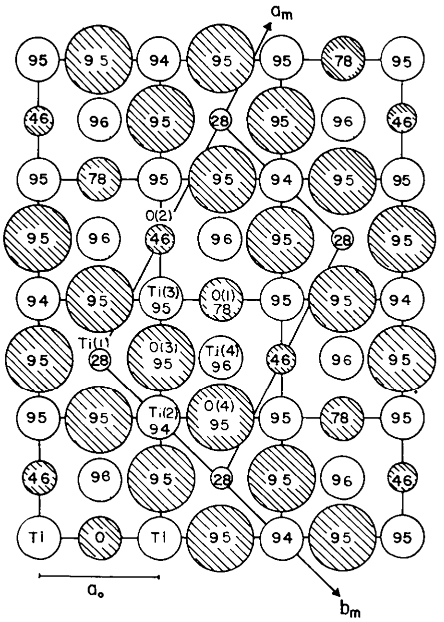

Fig. 2. The (001) plane in monoclinic TiO. Open circles and hatched circles show Ti and O ions respectively. $a_m$, $b_m$ are axes of the monoclinic cell. Here, $a_0$ is the lattice constant of the cubic cell. The numbers in the circles indicate percent occupation, and the sizes of circles are proportional to occupation factors.

---

* Scattering factors, including the dispersion corrections, were taken from *International Tables for X-ray Crystallography* (1962).

* The fully ordered phase probably contains vacancy waves with larger amplitudes, and fewer vacancies on planes parallel to the main wave. It was not possible to examine this state, because of the problems with domains mentioned earlier; this would be an interesting problem for studies by lattice imaging in the electron microscope.

Refinement was also attempted for the other two space groups consistent with the extinctions, *B*2 and *Bm*. In both cases the *y* and *z* parameters, which are fixed at $\frac{1}{2}$ in equipoints, 2(*b*), (*d*) in *B*2/*m*, refined to the value of 0·500.

Tests for the presence of interstitial ions were also made; an interstitial occupancy was included and all parameters but the temperature factors were allowed to vary. The refinement converged to small negative values for the interstitial occupation. This result is surprising since such interstitials are known to occur in FeO (Smuts, 1966; Roth, 1960; Koch & Cohen, 1969), (Ni,Co)O (Stiglich, Whitmore & Cohen, 1973) and VO (Morinaga & Cohen, 1976). To confirm this further, one crystal was quenched from 1050°C (above the ordering temperature) by pulling it to the cold zone of the furnace from this temperature. Some 17 fundamental peaks were integrated and refinement including interstitials is indicated in Fig. 3. (The temperature factors for Ti and O in this disordered phase are given in Table 1.) Again, there is not clear indication of interstitials.

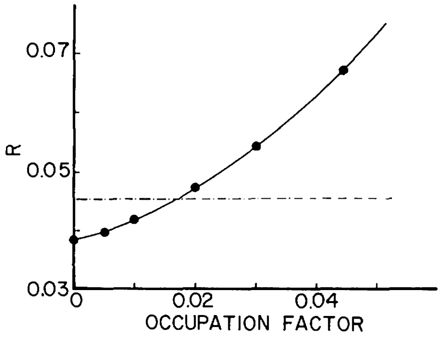

Fig. 3. *R* index *vs* Ti interstitial occupation factor in TiO. The horizontal dashed line represents 95% confidence limits, following Hamilton (1965*b*).

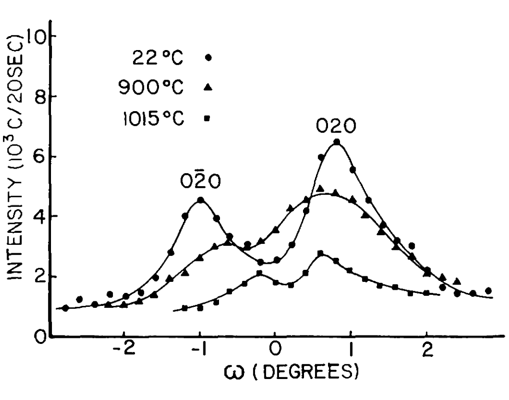

Fig. 4. ω scans near the 020 reflection in TiO at various temperatures.

## *Order vs temperature*

The intensity distribution in an ω scan near the 020 monoclinic reflection is shown in Fig. 4 for three temperatures. The reflections 020 and 0$\bar{2}$0 from two domains can be seen. The intensity decreases with increasing temperature and the splitting decreases. (It was found that equilibrium at each temperature required ~2 h.) The peak intensity of the 020 reflection *vs* temperature is given in Fig. 5. The 0$\bar{2}$0–020 splitting, $\delta\omega = 2\delta\gamma$ ($\delta\gamma \equiv 90° - \gamma_c$, $\gamma_c$ being the pseudo-cubic angle) is shown *vs* temperature in Fig. 6. From these two figures it is clear that the splitting and superlattice intensity are proportional and hence splitting is proportional to the square of the order parameter.

The transition temperature $T_c$ is 1026 (2)°C, 75°C above the temperature for continuous ordering (Terauchi & Cohen, 1977).

## Discussion

TiO is the first monoxide of the 3*d* transition elements that has been shown *not* to contain ions in interstitial

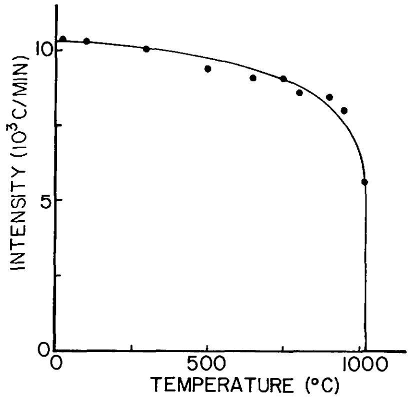

Fig. 5. Intensity of the 020 monoclinic reflection *vs* temperature.

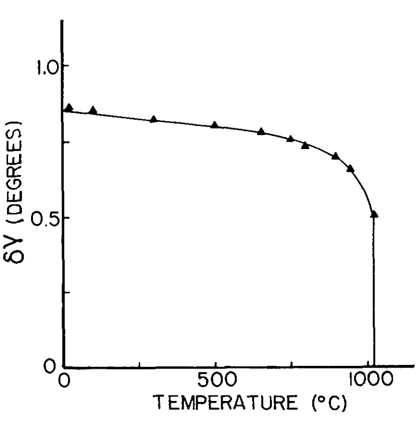

Fig. 6. $\delta\gamma = (90° - \gamma)$ in TiO *vs* temperature.

positions of the rock-salt structure. When the vacancies order, the structure is monoclinic and the average structure contains waves of vacancies every third (100) plane of the monoclinic phase, but there are vacancies on the planes in between as well. These 'waves' are somewhat different for the Ti and O ions, but in what follows we shall ignore this difference in a first attempt to understand the various interactions in this system that lead to the monoclinic distortion below $T_c$. We thus assume that there is one vacancy position (not a separate one on each sublattice) with average concentration $c$.

In a previous paper (Terauchi & Cohen, 1977) we have shown that the Hamiltonian for this system can be written in a mean-field approximation in terms of pair interactions and vacancy concentrations at a site $c_i$.

$$H = \tfrac{1}{2}\sum_{ij} J_{ij}(c_i - c)(c_j - c) + \frac{1}{\sqrt{N}}\sum_{j\mathbf{q}} G_{\mathbf{q}}(c_j - c)\,\rho_q \exp(i\mathbf{q}.\mathbf{r}_{ij}). \qquad (4)$$

Here the first term represents vacancy–vacancy interactions with energy $J_{ij}$ for sites $i$ and $j$ separated by $\mathbf{r}_{ij}$. The second term represents a vacancy–electron interaction, the exponent being a charge-density wave of wave vector $\mathbf{q}$ and amplitude $\rho_{\mathbf{q}}$. Writing the Fourier transformations of $J_{ij}$ as $J_{\mathbf{q}}$ and with the transform of $\sigma_i \equiv c_i - c$ as $\sigma_{\mathbf{q}}$:

$$H = \tfrac{1}{2}\sum_{\mathbf{q}} J_{\mathbf{q}}\sigma^*_{-\mathbf{q}}\sigma_{\mathbf{q}} + \sum_{\mathbf{q}} G_{\mathbf{q}}\sigma_{\mathbf{q}}\rho_{\mathbf{q}} = \tfrac{1}{2}\sum_{\mathbf{q}} J_{\text{eff}}(\mathbf{q})\sigma^*_{-\mathbf{q}}\sigma_{\mathbf{q}}, \qquad (5)$$

where we have assumed that $\rho_q$ is proportional to $\sigma_q$ as a result of screening. (TiO is a semiconductor.) The effective potential $J_{\text{eff}}(\mathbf{q})$ represents the difference in the (transformed) potentials, vacancy–vacancy minus vacancy–electron.

In the ordered phase, $\langle\sigma_{q_0}\rangle \equiv \sigma$. That is, the spatial average of $\sigma_q$ at the value of $\mathbf{q} = \mathbf{q}_o$, a superlattice position, does not vanish; it is an order parameter. The free energy per atom with $J_{\text{eff}} \equiv J_{\text{eff}}(\mathbf{q}_o)$ can then be written

$$F/N = \tfrac{1}{2}J_{\text{eff}}\sigma^2 + k_BT[\tfrac{1}{2}(1+\sigma)\log\tfrac{1}{2}(1+\sigma) + \tfrac{1}{2}(1-\sigma)\log\tfrac{1}{2}(1-\sigma)]. \qquad (6)$$

Here the second term is the entropy, which is assumed to be that of an Ising system. However, this expression does not include the distortion that has been shown to be coupled to ordering in this system. To include this coupling, we now expand the effective potential or ordering energy in terms of the strains, $e$:

$$J_{\text{eff}} = J^0_{\text{eff}} + \sum_{\alpha,\beta}\frac{\partial J_{\text{eff}}}{\partial e_{\alpha\beta}}e_{\alpha\beta}, \qquad (7)$$

where $\alpha$, $\beta$ represent coordinate axes, $x$,$y$,$z$. Also the temperature of continuous order is defined (from Terauchi & Cohen, 1977) as:

$$J^0_{\text{eff}} + k_BT_0 = 0. \qquad (8)$$

The distortion $\Delta\gamma = 90° - \gamma_c$ between the $a$ and $b$ axes is equivalent to a shear strain, $e_{xy}$. If other strain components are ignored for simplicity, the free energy may be written as:

$$F/N = \tfrac{1}{2}J^0_{\text{eff}}\sigma^2 + \tfrac{1}{2}J'_{\text{eff}}e_{xy}\sigma^2 + \frac{v}{2}C_{66}e^2_{xy} + K_BT[\tfrac{1}{2}(1+\sigma)\log\tfrac{1}{2}(1+\sigma) + \tfrac{1}{2}(1-\sigma)\log\tfrac{1}{2}(1-\sigma)]. \qquad (9)$$

Here $v$ is the volume of the unit cell and $C_{66}$ is the elastic constant for the shear $e_{xy}$. The third term represents the shear strain energy. The temperature dependence of both the order parameter and $\sigma$ and $e_{xy}$ are then determined from the stability conditions;

$$\frac{\partial F}{\partial\sigma} = \frac{\partial F}{\partial e_{xy}} = 0, \qquad (10)$$

which results in the following pair of equations:

$$e_{xy} = \frac{-J'_{\text{eff}}}{2C_{66}v}\sigma^2, \qquad (11a)$$

$$J^0_{\text{eff}}\sigma - \frac{J'^2_{\text{eff}}}{2C_{66}v}\sigma^3 + \tfrac{1}{2}k_BT\ln\left(\frac{1+\sigma}{1-\sigma}\right) = 0. \qquad (11b)$$

Equation (11*a*) shows that the strain is proportional to the square of the order parameter and hence to the intensity of a superlattice reflection, as is indicated by the experimental data. The temperature dependence of $\sigma$ (and hence the strain) is determined by (11*b*). The latter equation is most readily solved by defining two quantities:

$$X_1 = -J^0_{\text{eff}}\sigma + \frac{J'^2_{\text{eff}}}{2C_{66}v}\sigma^3, \qquad (12a)$$

$$X_2 = \tfrac{1}{2}k_BT\ln\left(\frac{1+\sigma}{1-\sigma}\right). \qquad (12b)$$

The value of $J^0_{\text{eff}}$ is 70·3 meV (Terauchi & Cohen, 1977). Therefore, $\sigma$ can be plotted *vs* $X_1$ from (12*a*) for various values of $J'^2_{\text{eff}}/2C_{66}v \equiv a$. Where this curve intersects $\sigma$ *vs* $X_2$ for a given $t/T_0$ determines the value(s) of $\sigma$. The results are shown schematically in Fig. 7. When $a = 0$, *i.e.* $J'_{\text{eff}} = 0$ (no strain coupling), $\sigma$ *vs* $T$ is continuous as is typical for a second-order phase transition. The temperature where $\sigma = 0$ is $T_0$. However, for $a = 1{\cdot}0\ k_BT_0$ there are two solutions for $\sigma$ indicating a first-order phase transition at $T_c = 1{\cdot}21\ T_0$. Thus the first-order nature of the transition in TiO appears to be explained by vacancy–strain coupling.

In Fig. 8, the data on order (peak intensity) and strain are shown *vs* temperature. The best fit to the data is obtained with $a = 0{\cdot}581\ k_B T_0$ which was chosen to give the value of $T_c = 1026\,°\mathrm{C}$ found in this study and the known $T_0 = 951\,°\mathrm{C}$ (Terauchi & Cohen, 1977), *i.e.* $T_c/T_0$ is known experimentally to be 1·062. The intensity ratio at $T_c$ is predicted to be 0·46, compared with the observed value of 0·57, and the actual strain at $T_c$, $\Delta\gamma = 0{\cdot}51°$, compared with the predicted value $\Delta\gamma = 0{\cdot}39°$.

Inserting (11*a*) into (9):

$$F = \tfrac{1}{2} J^0_{\mathrm{eff}} \sigma^2 - \tfrac{1}{4} a \sigma^4 + \text{entropy term.} \qquad (13)$$

The coefficient of the fourth power of $\sigma$ is negative, since $a > 0$. Thus, the free energy has a secondary minimum at a positive value of $\sigma$ in the range $T_0 < T < T_c$, as expected for a first-order transition. It is this fourth-power term in $\sigma$ that is causing the first-order transition (rather than the third-order term which is usually thought to be important in such cases). Also the reason for the appearance of domains is clear; the same minimum occurs at $\pm\sigma$.

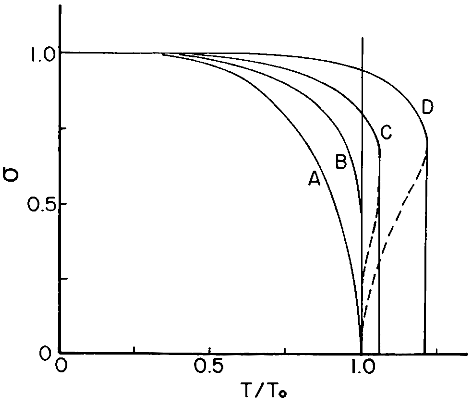

Fig. 7. Order parameter, $\sigma$, *vs* $T/T_0$ for various values of the constant, $a$: (*A*) $a = 0$, (*B*) $a = 0{\cdot}333\ k_B T_0$, (*C*) $a = 0{\cdot}581\ k_B T_0$, (*D*) $a = 1{\cdot}0\ k_B T_0$.

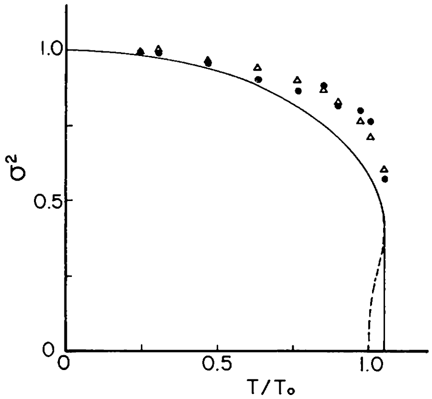

Fig. 8. Actual strain (triangles) and superlattice intensity (closed circles) *vs* $T$ and the theoretical curve $\sigma^2$ for $a = 0{\cdot}581\ k_B T_0$.

No evidence was found in this study made at high temperatures for the transition phase, reported by Watanabe *et al.* (1968, 1970); they employed quenched specimens.

The research was supported by the US Army Research Office under grant No. DAAG 29-76-G-0303. The X-ray work was carried out in the Long Term X-ray Facility of Northwestern University's Materials Research Center, supported in part by NSF through grant No. DMR 760157.

### References

Banus, M. D. & Reed, T. B. (1970). *The Chemistry of Extended Defects in Non-Metallic Solids*, edited by L. Eyring & M. O'Keeffe, pp. 488–522. Amsterdam: North-Holland.

Busing, W. R., Martin, K. O. & Levy, H. A. (1962). *ORFLS*. Report ORNL-TM-305 (as modified by J. Ibers). Oak Ridge National Laboratory, Tennessee.

Gehlen, P. C. (1969). *Rev. Sci. Instrum.* **40**, 715–718.

Hamilton, W. C. (1965*a*). *Acta Cryst.* **18**, 502–510.

Hamilton, W. C. (1965*b*). *Trans. Am. Crystallogr. Assoc.* **1**, 17–32.

*International Tables for X-ray Crystallography* (1962). Vol. III. Birmingham: Kynoch Press.

Koch, F. & Cohen, J. B. (1969). *Acta Cryst.* B**25**, 275–287.

Morinaga, M. & Cohen, J. B. (1976). *Acta Cryst.* A**32**, 387–395.

Reed, T. B. & Pollard, E. R. (1968). *J. Cryst. Growth*, **2**, 243–247.

Richesson, M., Morrison, L., Cohen, J. B. & Paavola, K. (1971). *J. Appl. Cryst.* **4**, 524–527.

Roth, W. L. (1960). *Acta Cryst.* **13**, 140–149.

Schwartz, L. H., Cohen, J. B. & Morrison, L. A. (1964). *Adv. X-ray Anal.* **7**, 281–301.

Smuts, J. (1966). *J. Iron Steel Inst. London*, **204**, 237–239.

Stiglich, J. J., Jr, Whitmore, D. H. & Cohen, J. B. (1973). *J. Am. Ceram. Soc.* **56**, 211–213.

Suortti, P. (1972). *J. Appl. Cryst.* **5**, 325–331.

Taylor, A. & Doyle, N. J. (1970). *The Chemistry of Extended Defects in Non-Metallic Solids*, edited by L. Eyring & M. O'Keefe, pp. 523–540. Amsterdam: North-Holland.

Terauchi, H. & Cohen, J. B. (1977). *J. Phys. Chem. Solids*. In the press.

Watanabe, D., Terasaki, O., Jostons, A. & Castle, J. S. (1967). *Acta Cryst.* **23**, 307–313.

Watanabe, D., Terasaki, O. Jostsons, A. & Castle, J. R. (1968). *J. Phys. Soc. Jpn*, **25**, 292.

Watanabe, D., Terasaki, O., Jostsons, A., & Castle, J. R. (1970). *The Chemistry of Extended Defects in Non-Metallic Solids*, edited by L. Eyring & M. O'Keeffe, pp. 238–258. Amsterdam: North-Holland.